

3-D Half-Spheroid Models for Transcranial Doppler Ultrasound Propagation Channels

Alexander Weir¹, Cheng-Xiang Wang² and Stuart Parks³

Abstract—In this paper, a method of characterization of a transcranial Doppler (TCD) ultrasound propagation channel is proposed. A simplified 3-D isotropic half-spheroid scattering channel model is described. The temporal autocorrelation function (ACF) is investigated. Based on the theoretical model, a sum-of-sinusoids (SoS) simulation model is proposed and its spatial-temporal properties are investigated.

I. INTRODUCTION

TCD ultrasound [1] is used to interrogate the intracranial arterial system for detection of micro embolic signals (MES) for the diagnosis and prediction of embolic complications in stroke-risk patients. MES detection is a mature application of Doppler ultrasound. When detected, emboli produce unidirectional high intensity transient signals (HITS) which give a distinctive 'popping' sound when observed. Due to the complexities of their formation, emboli can be corpuscular (e.g lipid droplets, calcified particles etc.) or gaseous (e.g. artificially inserted gas or as the result of microcavitation). Currently it is difficult to robustly detect all MES.

A close examination of the TCD ultrasound propagation channel will benefit and improve our understanding of the received signals in TCD. A simplified stochastic SoS channel simulator can provide a platform for efficient analysis of multi-path effects, in terms of reflection, refraction, diffraction and scattering in the ultrasound propagation channel.

This paper is organized as follows: Section II describes the 3-D half-spheroid theoretical reference model in terms of its geometry, leading to the development of the probability distribution function (PDF) in both azimuth and elevation angles of arrival. Section III describes the characteristics of the theoretical model and provides a closed form expression for the ACF. In Section IV, using the theoretical 3-D hemispherical model as a mathematical reference, we derive the corresponding SoS simulation model and determine its parameters. Section V examines the performance of the simulated model and the paper concludes in Section VI.

¹A. Weir is with the Medical Devices Unit, Department of Clinical Physics, Southern General Hospital, Glasgow, United Kingdom and the School of Engineering and Physical Science, Heriot-Watt University, Edinburgh, United Kingdom. alexander.weir@nhs.net

²C.-X. Wang is with School of Engineering and Physical Science, Heriot-Watt University, Edinburgh, United Kingdom. cheng-xiang.wang@hw.ac.uk

³S. Parks is with the Medical Devices Unit, Department of Clinical Physics, Southern General Hospital, Glasgow, United Kingdom. stuart.parks@nhs.net

II. THEORETICAL REFERENCE MODEL

A. Model Geometry

The study of multipath effects and design of wireless communications systems has evolved through many theoretical 2-D and 3-D channel models [2]-[4]. By considering the envelope correlation for a fading channel in ultrasound to be analogous to that of an unmodulated carrier in a mobile communications system, we can apply such developments to the characterization of a Doppler ultrasound propagation channel.

In this study, the scattering geometry can be elaborated by considering the propagation channel as a 3-D isotropic half-spheroid model [5]-[8], as shown in Fig. 1. The transducer is assumed to be stationary and positioned at the origin of the Cartesian coordinates. The ultrasound system is simplified to consider only the returning reflection from a strong scattering region within blood flow of an insonated vessel. Strong scatterers are assumed to exist within and around the periphery of the half-spheroid region. The intersection of the scatterers with the xz -plane is a semi-ellipse with axial length $2a$ and b along the x and z axis respectively [8]. The direction of blood flow in the insonation region is, without any loss of generality, assumed to be in the direction of the x -axis with velocity v . Tissue is assumed to be homogeneous with uniform acoustic impedance. The ultrasound pulse is transmitted by a transducer. Echoes received from stationary tissue can be considered to exhibit the same frequency and phase as the transmitted signal. Echoes from scatterers (i.e. moving tissue and fluids) will exhibit slight differences in delay and/or phase. From these differences the Doppler frequency is obtained which can then be processed to produce a Doppler sonogram. The complex received signal is subjected to a number of propagation effects. The backscattered signal may be refracted or diffracted by tissue objects in and around the insonation path, or reflected at tissue boundaries.

The channel response in this multi-path fading channel comprises of N propagation paths and can be expressed as [5]

$$g(t) = \sum_{i=1}^N C_n e^{j\theta_n(t)}, \quad (1)$$

where

$$\theta_n(t) = \theta_n - 2\pi [(f_c + f_{D_n}) \tau_n - f_{D_n} t], \quad (2)$$

is the time-variant phase associated with the n^{th} path. In (2), phase shift θ_n is randomly introduced by the scatterer and can be uniformly distributed between $-\pi$ and π , τ_n is

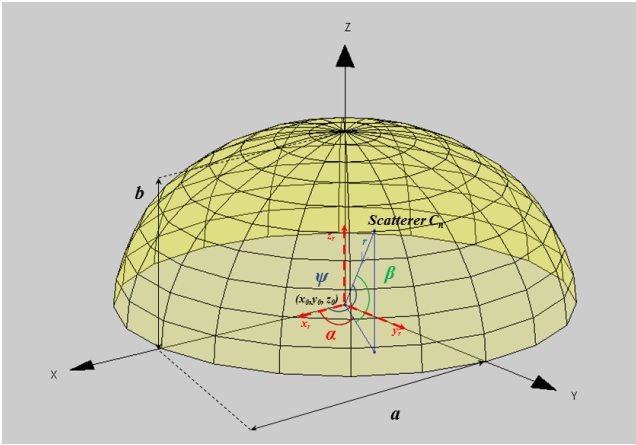


Fig. 1. An illustration of the 3-D plane within a hemispherical model.

the time delay of the n^{th} propagation path, C_n is the signal amplitude, f_c is the ultrasound insonation frequency and f_{D_n} is the Doppler shift. The magnitude of C_n depends on the cross sectional area of the scatterer and its properties; most usually blood, since erythrocytes (red blood cells) are the most significant scattering bodies in the insonation region. The received band pass signal may be expressed as

$$\begin{aligned} r(t) &= \text{Re}[g(t)e^{j2\pi f_c t}] \\ &= \text{Re}[(g_I(t) + jg_Q(t)) \cdot (\cos(2\pi f_c t) + j\sin(2\pi f_c t))], \end{aligned} \quad (3)$$

where the in-phase and quadrature components $g_I(t)$ and $g_Q(t)$ are

$$g_I(t) = \sum_{i=1}^N C_n \cos(\theta_n(t)) \quad (4)$$

and

$$g_Q(t) = \sum_{i=1}^N C_n \sin(\theta_n(t)). \quad (5)$$

Each plane wave has an angle of arrival (AOA). The spatial AOA ψ_n is the angle formed between the incident wave and the direction of motion of blood flow and consists of two components; an azimuth angle of arrival (AAOA) α_n to the x-z plane and an elevation angle of arrival (EAOA) β_n to the x-y plane. The model parameters α_n , β_n , θ_n and C_n are all random and statistically independent. The n^{th} incident plane wave in a 3-D plane can be described by

$$E_n(t) = C_n e^{j(\theta_n t - k\hat{A})}, \quad (6)$$

where

$$\hat{A} = [x_0 \cos(\alpha) \cos(\beta) + y_0 \cos(\alpha) \sin(\beta) + z_0 \sin(\beta)] \quad (7)$$

and k is the wave propagation constant determined by

$$k = \frac{2\pi}{\lambda_c}. \quad (8)$$

The sum of N statistically independent plane waves is given by

$$E(t) = \sum_{n=1}^N E_n(t). \quad (9)$$

B. Probability Distribution Function (PDF)

The PDFs of AAOA and EAOA, i.e. $p_\alpha(\alpha)$ and $p_\beta(\beta)$, can be used to define the PDF of the spatial AOA, $p_\psi(\psi)$.

As shown in [7] and [8], with the assumption that scatterers are distributed uniformly around the transducer, the PDF of the AAOA, $p_\alpha(\alpha)$, is

$$p_\alpha(\alpha) = \frac{1}{2\pi}, 0 \leq \alpha \leq 2\pi \quad (10)$$

and the PDF of the EAOA, $p_\beta(\beta)$, is

$$p_\beta(\beta) = \frac{\left(\frac{b}{a}\right)^2 \cos(\beta)}{\left[\sin^2(\beta) + \left(\frac{b}{a}\right)^2 \cos^2(\beta)\right]^{\frac{3}{2}}}, 0 \leq \beta \leq \frac{2}{\pi}. \quad (11)$$

The PDF of EAOA can be seen to depend only on the ratio of $\frac{b}{a}$, and for the special case where $a = b$ the PDF simplifies to $p_\beta(\beta) = \cos(\beta)$. The PDF of EAOA is shown as a function of the elevation angle for sample values of $\frac{b}{a}$ in the case of an oblate spheroid ($b \leq a$) in Fig. 2 and a prolate spheroid ($b \geq a$) in Fig 3. In this investigation we consider variations in the ratio of $\frac{b}{a}$ as it is unclear at this juncture which ratio may best match measured results.

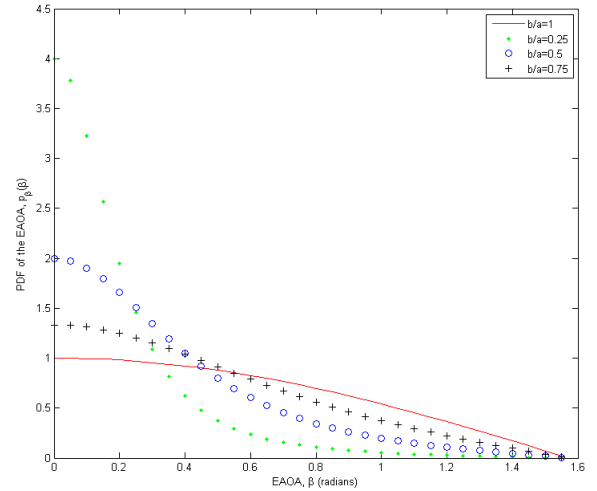


Fig. 2. The PDF of the EAOA seen at the transducer for $\frac{b}{a} = 0.25, 0.5, 0.75$ and 1, (i.e. an oblate half spheroid).

III. THEORETICAL MODEL CHARACTERISTICS

The characteristics of the theoretical model are investigated in this section in terms of the temporal ACF. The ACF, $\phi_{rr}(\tau)$, is defined as the ensemble average $E[\cdot]$ of the product of $r(t)$ with itself at a time separation τ when $r(t)$ is wide-sense stationary (WSS) [5], which in turn imposes the condition that

$$\phi_{g_I g_I} = \phi_{g_Q g_Q} \text{ and } \phi_{g_I g_Q} = -\phi_{g_Q g_I}. \quad (12)$$

It can be shown that the ACF is the integral of the product of the baseband signal and the joint density function [8],

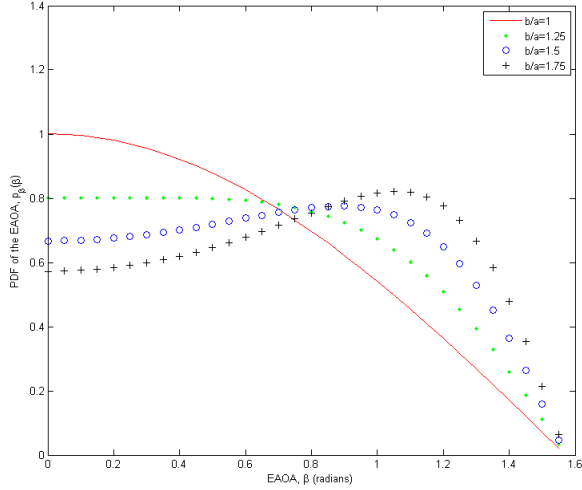


Fig. 3. The PDF of the EAOA seen at the transducer for $\frac{b}{a} = 1, 1.25, 1.5,$ and 1.75 (i.e. a prolate half spheroid).

given by

$$\phi_{rr}(\tau) = \frac{\Omega_p}{2} \int_0^{\frac{\pi}{2}} J_0(2\pi f_m \tau \cos \beta) \cdot \left[\frac{\left(\frac{b}{a}\right)^2 \cos(\beta)}{\left[\sin^2 \beta + \left(\frac{b}{a}\right)^2 \cos^2 \beta\right]^{\frac{3}{2}}} \right] d\beta, \quad (13)$$

where Ω_p is the total received power, f_m is the maximum Doppler frequency, β is the EAOA and $J_0(\cdot)$ denotes the zeroth-order Bessel function of the first kind. The theoretical temporal ACF is shown in Fig. 4 for $\frac{b}{a}$ values of 0.5, 0.75, 1, 1.25 and 1.5, representing a range of oblate and prolate half-spheroid models and Ω_p has been normalised.

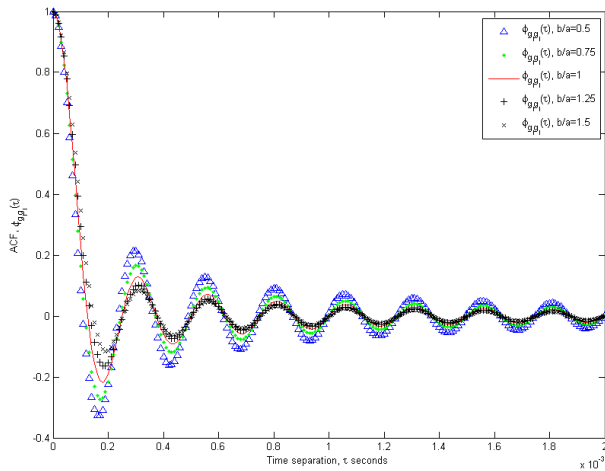


Fig. 4. The theoretical ACF of the 3-D half-spheroid model for $\frac{b}{a} = 0.5, 0.75, 1, 1.25,$ and 1.5 .

IV. THE SIMULATION MODEL

In this section a SoS simulation model is proposed. The simulation model emulates signals received at the transducer in a TCD ultrasound system using the theoretical half-spheroid model as a reference. The emulated receive signal $\hat{g}(t)$ has in-phase and quadrature components such that

$$\hat{g}(t) = \hat{g}_I(t) + j\hat{g}_Q(t) = \hat{g}_1(t) + \hat{g}_2(t). \quad (14)$$

The channel simulators Gaussian process $\hat{g}_i(t)$ can be approximated by

$$\hat{g}_i(t) = \sum_{n=1}^N C_{i,n} \cos(2\pi f_{i,n} t + \theta_{i,n}), i = 1, 2, \quad (15)$$

where $C_{i,n}$ represents the gains, $(2\pi f_{i,n} t)$ the Doppler frequencies and $\theta_{i,n}$ the phases of N respective exponential functions.

A. Simulation Model Parameters

The simulation model parameters must be determined such that the process given by (15) has the desired statistics. In this study, the Method of Exact Doppler Spread (MEDS) is used to compute these statistics. The parameters in (15) can be generated using the following expressions;

$$C_{i,n} = \sigma \sqrt{\frac{2}{N}}, \quad (16)$$

$$f_{i,n} = f_{D_{max}} \cos \psi_n = f_{D_{max}} \cos \alpha_n \cos \beta_n, \quad (17)$$

$$\text{and } \theta_{i,n} = 2\pi \frac{n}{rand(1:N)}. \quad (18)$$

The values for $f_{D_{max}}$ and σ are identical to the reference model. These parameters are kept constant during the simulation and the model statistical properties are derived by using time averaging instead of statistical averaging.

B. Temporal ACF

The closed form expression for the simulated ACF is given by [8] as

$$\hat{\phi}_{rr}(\tau) = \sum_{n=1}^N \frac{C_n^2}{2} \cos(2\pi f_{D_{max}} \cos \alpha_n \cos \beta_n \tau) \quad (19)$$

The parameters α_n and β_n must be evaluated for the simulation model such that the theoretical and simulated temporal ACFs are a close match. These parameters can be determined using an error minimising function, such as the Lp-norm method [9]. The parameter β_n can be found using the closed form expressions for the theoretical and simulated spatial cross-correlation function (CCF) [8], given as

$$\hat{\rho}(D) = \int_0^{\frac{\pi}{2}} \exp(j2\pi \frac{D}{\lambda} \sin \beta) p_\beta(\beta) d\beta \quad (20)$$

and

$$\hat{\rho}(D) = \frac{1}{N} \sum_{n=1}^N e^{-j2\pi \frac{D}{\lambda} \sin \beta_n}. \quad (21)$$

Using an arbitrary spatial separation of an integral number of wavelengths, parameter β_n can be evaluated using the error function

$$E_1^{(p)} = \left[\int_0^{D_{max}} |\rho(D) - \hat{\rho}(D)|^p dD \right]^{\frac{1}{p}}. \quad (22)$$

Similarly, the parameter α_n can be calculated using the Lp-norm error function

$$E_2^{(p)} = \left[\int_0^{\tau_{max}} |\phi_{rr}(\tau) - \hat{\phi}_{rr}(\tau)|^p d\tau \right]^{\frac{1}{p}}. \quad (23)$$

V. RESULTS

The performance of the theoretical reference model and the simulation model is shown in fig. 5 and fig. 6. In fig. 5 the theoretical and simulated temporal ACFs for various $\frac{b}{a}$ ratios of the 3-D half-spheroid model and model parameters $f_{D_{max}} = 4$ KHz, $\sigma^2 = 1$, $N = 30$ and $\tau_{max} = 0.012$ s are shown. The plots of temporal ACF for the reference model and simulation model show good agreement for each variation in the reference model geometry. In fig. 6 the theoretical and simulated spatial CCF for the 3-D half-spheroid model with ratios $\frac{b}{a}$ and model parameters $f_{D_{max}} = 4$ KHz, $\sigma^2 = 1$, $N = 30$ and $D_{max} = 4\lambda$ is shown. The plots of spatial CCF for the reference model and simulation model again show good agreement.

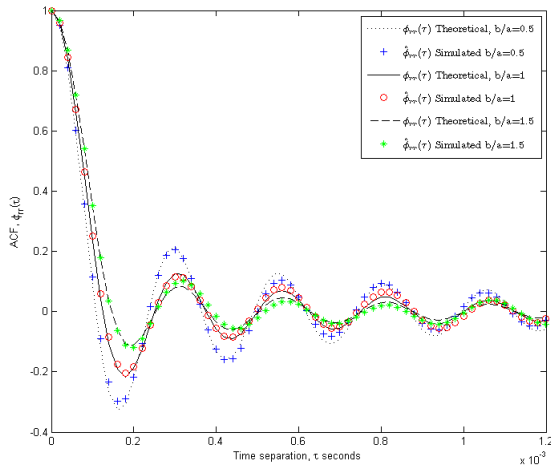


Fig. 5. A plot of the theoretical and simulated temporal ACFs for various $\frac{b}{a}$ ratios of the 3-D half-spheroid model, $f_{D_{max}} = 4$ KHz, $\sigma^2 = 1$, $N = 30$ and $\tau_{max} = 0.012$ s.

VI. CONCLUSIONS

In this paper, a 3-D half-spheroid theoretical model has been proposed for investigation of the characteristics of a TCD ultrasound propagation channel based on methods developed for stochastic analysis of mobile communications systems. The characteristics of the theoretical model have been investigated and closed form expressions have been

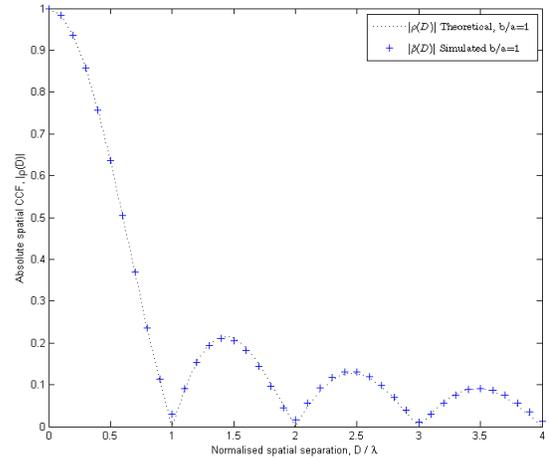


Fig. 6. A plot of the theoretical and simulated spatial CCFs for the 3-D half-spheroid model with ratio $\frac{b}{a} = 1$, $f_{D_{max}} = 4$ KHz, $\sigma^2 = 1$, $N = 30$ and $D_{max} = 4\lambda$.

derived for the PDFs and ACF. Using the theoretical model as a reference, a SoS simulation model has been proposed. The statistical properties of the simulation model are developed using MEDS and the Lp-norm error minimising function to ensure the ACF of the simulation is as close as possible to the theoretical reference. This is demonstrated in the results, which show a close fit between the theoretical mathematical reference model and the simulation model. The next stage in this research will complete the second order statistical analysis by considering the Doppler PSD, level crossing rate (LCR) and average fade duration (AFD). The validity of the theoretical and simulation models will then be tested through comparison with measured results using a custom Doppler phantom.

REFERENCES

- [1] M.S. Markus. Transcranial Doppler ultrasound. *J Neurol Neurosurg Psychiatry*, vol. 67, pp. 135-137, 1999.
- [2] W.C. Jakes. (Ed.) *Microwave Mobile Communications*. New Jersey: IEEE Press, 1994.
- [3] R.H. Clarke. "A statistical theory of mobile-radio reception," *Bell Syst. Tech. J.*, vol. 47, pp. 957-1000, 1968.
- [4] T. Aulin. "A modified model for the fading signal at a mobile radio channel." *IEEE Trans. Veh. Technol.*, vol. 28, no. 3, pp. 182-203, 1979.
- [5] G.L. Stüber. *Principles of Mobile Communications, Second Edition*. Boston: Kluwer Academic Publishers, 2001.
- [6] Q. Yao and M. Pätzold. "A novel 3-D spatial-temporal deterministic simulation model for mobile fading channels." *IEEE Int. Sym. On Personal, Indoor and Mobile Radio Communications (PIMRC03)*, Beijing, China, Sept. 2003, pp. 1506-1510.
- [7] R. Janaswamy. "Angle of arrival statistics for a 3-D spheroid model." *IEEE Trans. Veh. Technol.*, vol. 51, no. 5, pp. 1242-1247, Sept. 2002.
- [8] Q. Yao and M. Pätzold. "Spatial-Temporal Characteristics of a Half-Spheroid Model and its Corresponding Simulation Model." *IEEE 59th Vehicular Technology Conference, VTC 2004-Spring*, 1, 147151.
- [9] M. Pätzold. *Mobile Fading Channels*. Chichester, UK: John Wiley and Sons, 2002.